Serial clustering of extratropical cyclones over the North Atlantic and Europe under recent and future climate conditions

Serial clustering of extratropical cyclones over the North Atlantic and Europe under recent and future climate conditions

Joaquim G. Pinto,[1,2] Nina Bellenbaum,[2] Melanie K. Karremann,[2] and Paul M. Della-Marta[3]

Received 18 July 2013; revised 24 October 2013; accepted 28 October 2013; published 22 November 2013.

[1] Under particular large-scale atmospheric conditions, several windstorms may affect Europe within a short time period. The occurrence of such cyclone families leads to large socioeconomic impacts and cumulative losses. The serial clustering of windstorms is analyzed for the North Atlantic/western Europe. Clustering is quantified as the dispersion (ratio variance/mean) of cyclone passages over a certain area. Dispersion statistics are derived for three reanalysis data sets and a 20-run European Centre Hamburg Version 5 /Max Planck Institute Version–Ocean Model Version 1 global climate model (ECHAM5/MPI-OM1 GCM) ensemble. The dependence of the seriality on cyclone intensity is analyzed. Confirming previous studies, serial clustering is identified in reanalysis data sets primarily on both flanks and downstream regions of the North Atlantic storm track. This pattern is a robust feature in the reanalysis data sets. For the whole area, extreme cyclones cluster more than nonextreme cyclones. The ECHAM5/MPI-OM1 GCM is generally able to reproduce the spatial patterns of clustering under recent climate conditions, but some biases are identified. Under future climate conditions (A1B scenario), the GCM ensemble indicates that serial clustering may decrease over the North Atlantic storm track area and parts of western Europe. This decrease is associated with an extension of the polar jet toward Europe, which implies a tendency to a more regular occurrence of cyclones over parts of the North Atlantic Basin poleward of 50°N and western Europe. An increase of clustering of cyclones is projected south of Newfoundland. The detected shifts imply a change in the risk of occurrence of cumulative events over Europe under future climate conditions.

Citation: Pinto, J. G., N. Bellenbaum, M. K. Karremann, and P. M. Della-Marta (2013), Serial clustering of extratropical cyclones over the North Atlantic and Europe under recent and future climate conditions, *J. Geophys. Res. Atmos.*, *118*, 12,476–12,485, doi:10.1002/2013JD020564.

1. Introduction

[2] Between late December 2006 and mid January 2007, a rapid sequence of intense windstorms hit the North Atlantic Basin and Europe. Its most prominent storm "Kyrill" (cyclone name as given by the Free University-Berlin and used by the German Weather Service) affected large parts of Europe, caused a large socioeconomic impact, and claimed 47 lives [cf. *Fink et al*., 2009]. Windstorms are in fact the main natural hazard affecting Europe in terms of insured losses, and several previous studies have estimated both return periods and associated losses [e.g., *Della-Marta et al*., 2009, 2010; *Schwierz et al*., 2010; *Haylock*, 2011; *Pinto et al*., 2012]. An important result is that large cumulative (annual) losses can be attributed to the occurrence of multiple windstorms within a year (or season): The total damage attributed to the storms series of 1990, 1999, and 2007 ranks among the highest of the recent decades, with total costs reaching 10, 18, and 10 billion U.S. dollars in terms of insured losses [*MunichRe*, 2010].

[3] Recent studies on serial clustering of extratropical windstorms [e.g., *Mailier et al*., 2006] discuss two physical mechanisms that may contribute to the clustering process. First, groups of storms typically occur when successive unstable waves develop and move rapidly along the trailing front in the wake of a large "parent" or "primary" low, leading to the occurrence of cyclone families [e.g., *Bjerknes and Solberg*, 1922]. Such a phenomena is called secondary cyclogenesis, and the new cyclone typically appears south of the primary low [e.g., *Parker*, 1998; *Rivals et al*., 1998; *Dacre and Gray*, 2009]. Second, the large-scale atmospheric conditions play a crucial role on the incidence of storm series. The variability of extratropical cyclone tracks and intensities are linked with teleconnection patterns [e.g., *Raible*, 2007; *Seierstad et al*., 2007; *Bader et al*., 2011; *Franzke*, 2013]. Over the eastern North Atlantic/western Europe, the steering of cyclone tracks is largely associated with the phase of the North Atlantic Oscillation [e.g., *Hurrel et al*., 2003], which

Additional supporting information may be found in the online version of this article.

[1]Department of Meteorology, University of Reading, Reading, UK.
[2]Institute for Geophysics and Meteorology, University of Cologne, Cologne, Germany.
[3]Partner Reinsurance Company, Zurich, Switzerland.

Corresponding author: J. G. Pinto, Department of Meteorology, University of Reading, Earley Gate, PO Box 243, Reading RG6 6BB, UK. (j.g.pinto@reading.ac.uk)

2169-897X/13/10.1002/2013JD020564

effectively modulates the large-scale factors relevant for cyclone development [cf. *Pinto et al*., 2009]. For example, the large-scale flow in early 2007 showed a quasi-stationary zonal, stronger than average, upper air and surface flow with enhanced baroclinicity over the whole North Atlantic/Europe [*Fink et al*., 2009]. These atmospheric conditions supported the development and propagation of a succession of extratropical cyclones following a very similar path, including some high impact storms like "Franz," "Hanno," and "Kyrill" (11, 14, and 18 January 2007, respectively). *Mailier et al*. [2006] summarizes that the observed cyclone clusters are caused by a combination of inhomogeneous (steering through large-scale patterns) and cluster processes (secondary cyclogenesis). Thus, the occurrence of a fast succession of storms is not uncommon in meteorological terms but associated with rather specific large-scale atmospheric conditions.

[4] An important question is whether clustering of extratropical cyclones may change under future climate conditions. In general terms, the total number of cyclones is expected to decrease, while the number of extreme cyclones over western Europe may actually slightly increase in association with an intensified and eastward extended polar jet toward Europe [e.g., *Bengtsson et al*., 2006; *Pinto et al*., 2009; *Ulbrich et al*., 2009; *Zappa et al*., 2013b]. In accordance, shorter return periods for extreme windstorms and associated losses have been estimated for western Europe [*Della-Marta and Pinto*, 2009; *Pinto et al*., 2012]. In conjunction with the eddy-driven jet stream changes [e.g., *Delcambre et al*., 2013b], the North Atlantic Oscillation phase is expected to shift to a more dominant positive phase with enhanced greenhouse gas forcing, even though the physical reasons for this change are still under discussion [e.g., *Rind et al*., 2005; *Stephenson et al.*, 2006; *Bader et al*., 2011]. However, little attention has been paid to analyzing to what extent the clustering of extratropical cyclones may change under future climate conditions. The only known study is that of *Mailier* [2007], which considered three global climate models (GCMs) and found strong disagreement between the simulations.

[5] The first objective of this work is to analyze whether clustering of cyclones is a robust feature in the various reanalysis data sets and to investigate to what extent it is dependent on intensity. Second, the representation of cyclone clustering in a large ensemble of GCM simulations is analyzed in order to estimate the variability of clustering under recent climate conditions and possible changes in future decades.

2. Data and Methods

[6] Three reanalysis data sets are used in this study: (a) National Centers for Environmental Prediction (NCEP)/National Center for Atmospheric Research reanalysis (1948–2012; hereafter NCEP [*Kistler et al*., 2001]), with a spectral horizontal resolution of T62 (approximately 1.9°); (b) European Centre for Medium-Range Weather Forecasts 40 year reanalysis (1958–2002, hereafter ERA-40; *Uppala et al*. [2005]), with T106 resolution (approximately 1.125°); and (c) ERA-Interim reanalysis (1979–2012; hereafter ERAI, *Dee et al*. [2011]), with T255 (approximately 0.75°) resolution. To permit a better comparison between data sets and to maintain consistency of the cyclone tracking parameters, we reduced the spectral resolution of ERA-40 and ERAI to that of NCEP by removing all wave numbers higher than T62 [cf. *Pinto et al*., 2005]. This is important as the spectral truncation leads to more comparable cyclone numbers and intensity statistics with NCEP [*Jung et al*., 2006], although the representation of physical processes associated with cyclones still differs. Mean sea level pressure (MSLP) data were converted to 2.5° resolution.

[7] A large ensemble of simulations with the coupled ECHAM5/MPI-OM1 GCM (European Centre Hamburg Version 5 /Max Planck Institute Version–Ocean Model Version 1; [*Jungclaus et al*., 2006]; hereafter ECHAM5) at T63 resolution (approximately 1.9°) is considered. These ensemble simulations are forced with the historical greenhouse gas and aerosol concentrations for the period 1860–2000 (20C) and with the Special Report on Emissions Scenarios scenario A1B for the period 2001–2100. Three simulations were performed by the MPI in Hamburg for Coupled Model Intercomparison Project phase 3 (CMIP3) [*Jungclaus et al*., 2006]. The other runs were computed for the Ensemble Simulations of Extreme Weather Events Under Nonlinear Climate Change (ESSENCE) project [*Sterl et al*., 2008] by the Royal Dutch Meteorological Institute (KNMI). In total, 40 ensemble simulations are used, 20 for the 20th century period (1960–2000) and 20 for the end of the 21st century (2060–2100). This latter period was chosen as it corresponds to a time window when the influence of greenhouse gas forcing to cyclone activity can be clearly identified [e.g., *Ulbrich et al*., 2009; *Zappa et al*., 2013b]. The choice of a large ensemble with a single GCM rather than a multimodel ensemble like CMIP5 [*Taylor et al*., 2012] is motivated by the focus (as a first step) on testing the statistical robustness and applicability of the method rather than to analyze the intermodel dependency and climate sensitivity. The identified changes in synoptic activity for ECHAM5 under future climate conditions are close to the CMIP3 ensemble average [*Ulbrich et al*., 2008] and are very similar in terms of the spatial pattern to the CMIP5 ensemble average [*Harvey et al*., 2012]. Results presented here may be seen as representative for a larger ensemble, even though uncertainty is surely underestimated.

[8] Cyclones are identified and tracked using an automatic algorithm developed by *Murray and Simmonds* [1991a, 1991b], which was adapted for the Northern Hemisphere cyclone characteristics [*Pinto et al*., 2005]. Six-hourly MSLP data is used as an input. The method identifies and tracks cyclones based on a proxy of their relative geostrophic vorticity [cf. *Murray and Simmonds*, 1991a], which is approximated by the Laplacian of MSLP. The tracking methodology performs well in comparison to other similar techniques [*Neu et al*., 2013]. As this method is different from the approach of *Hodges* [1995], which was used in former studies on clustering [e.g., *Mailier et al*., 2006; *Vitolo et al*., 2009], the sensitivity of clustering to the choice of tracking methods can also be evaluated to some extent. In a previous study, *Della-Marta and Pinto* [2009] showed that the distribution of cyclone core pressure is well represented in ECHAM5 compared to NCEP and ERA-40, unlike vorticity, which is systematically too weak in the GCM for storms over the North Atlantic and western Europe. We chose to use minimum core MSLP as a measure of cyclone intensity, as it is a more robust and spatially consistent variable less affected by small-scale maxima than low-level vorticity [*Ulbrich et al*., 2009]. In order to avoid the drawbacks of MSLP as intensity measure [e.g., *Ulbrich et al*., 2009] and to take the projected changes in the background MSLP field into account [cf. *Hueging*

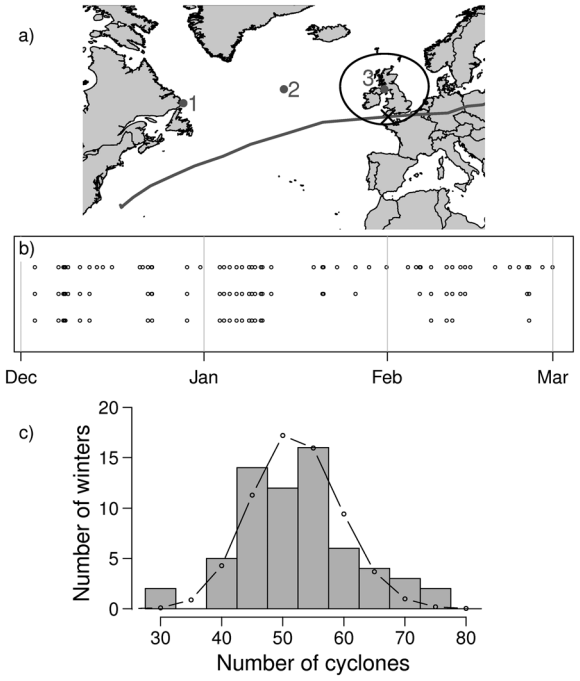

Figure 1. (a) Study area of the North Atlantic region and location of selected grid points (grid point 1: 52.5°N, 55°W; grid point 2: 55°N, 30°W; and grid point 3: 55°N, 5°W). The circular line around grid point 3 (with radius 700 km) corresponds to the area considered to count cyclone passages around this grid point. (b) Occurrence of cyclone passages for grid point 3 during the period December 1957 to February 1958 for different intensity thresholds: upper row: all cyclones, middle row: cyclones with minimum core pressure exceeding the 90th percentile, and lower row: cyclones with minimum core pressure exceeding the 95th percentile. (c) Number of cyclone passages per winter (December–February) and theoretical Poisson distribution (curve) for grid point 3.

et al., 2013; their Figure 6a], the percentiles are calculated separately for 1960–2000 and 2060–2100.

[9] The clustering of events can be quantified using a statistical approach. A point process [*Cox and Isham*, 1980] is used to model the sequence of incidences. The simplest model, which describes complete serial randomness, is the homogeneous one-dimensional Poisson process. This process can be used to describe the temporal distribution of events at a fixed location. By defining a cyclone passage near a certain location as an event, the succession of cyclone events can be considered as an inhomogeneous one-dimensional Poisson process [*Mailier et al*., 2006].

[10] The Poisson distribution which describes the random existence of events in a Poisson process is used to evaluate the statistical characteristics of cyclone occurrences with variance Var(N) and mean of number of events $E(N)$ per time interval. Following the work of *Mailier et al*. [2006], we consider the dispersion statistics, defined as the coefficient of variation (Var(N)/$E(N)$) minus one:

$$\Psi = \mathrm{Var}(N)/E(N) - 1$$

[11] For a Poisson distributed random variable, $E(N)$ is equal to Var(N) and so $\Psi = 0$. In this case, cyclone occurrences are randomly distributed. Positive results ($\Psi > 0$) denote overdispersion and correspond to a clustered process and/or a rate-varying process. A negative value ($\Psi < 0$) indicates underdispersion and therefore to a regular process. *Vitolo et al*. [2009] showed a general increase in Ψ with increasing aggregation period. Following their evaluation, we have selected an aggregation period of 3 month counts (December to February) to estimate Ψ for our cyclone statistics.

[12] Unlike previous studies [*Mailier et al*., 2006; *Kvamsto et al*., 2008; *Vitolo et al*., 2009], we consider cyclone tracks independently from their moving direction by defining a radius of influence around a grid point. This choice is inspired by the methodology to compute track density in the *Murray and Simmonds* [1991a, 1991b] algorithm and is similar to the approach used by *Mumby et al*. [2011] for tropical cyclones. Using a circle allows a points' clustering statistics to be influenced by cyclones whose tracks did not traverse a set longitude. If a cyclone track intercepts with the circle, it is counted at the time where its location is nearest to the circle center (Figure 1a), and the minimum core pressure within the circle is recorded for evaluation. The choice of radius is an important issue: if the radius is too small, influential cyclones are possibly not considered, and the counts may become random. On the other hand, if the chosen value is too

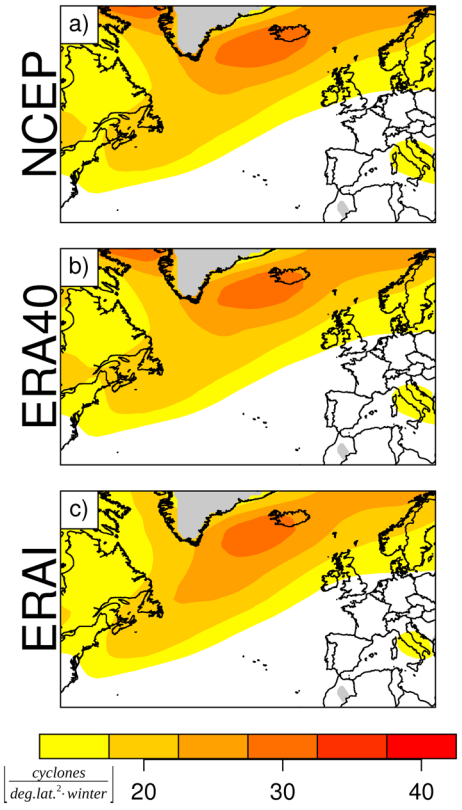

Figure 2. (a) Cyclone track density for NCEP for winter season (December–February) for the period 1948–2012. Values given in cyclone days per winter (December–February) per (degree latitude)^2. (b) Same as Figure 2a but for ERA-40 for the period 1958–2002. (c) Same as Figure 2a but for ERAI for the period 1979–2011. ERA-40 and ERAI data were spectrally degraded to T62 to enable direct comparison. Values in areas with orography above 1500 m are suppressed (gray).

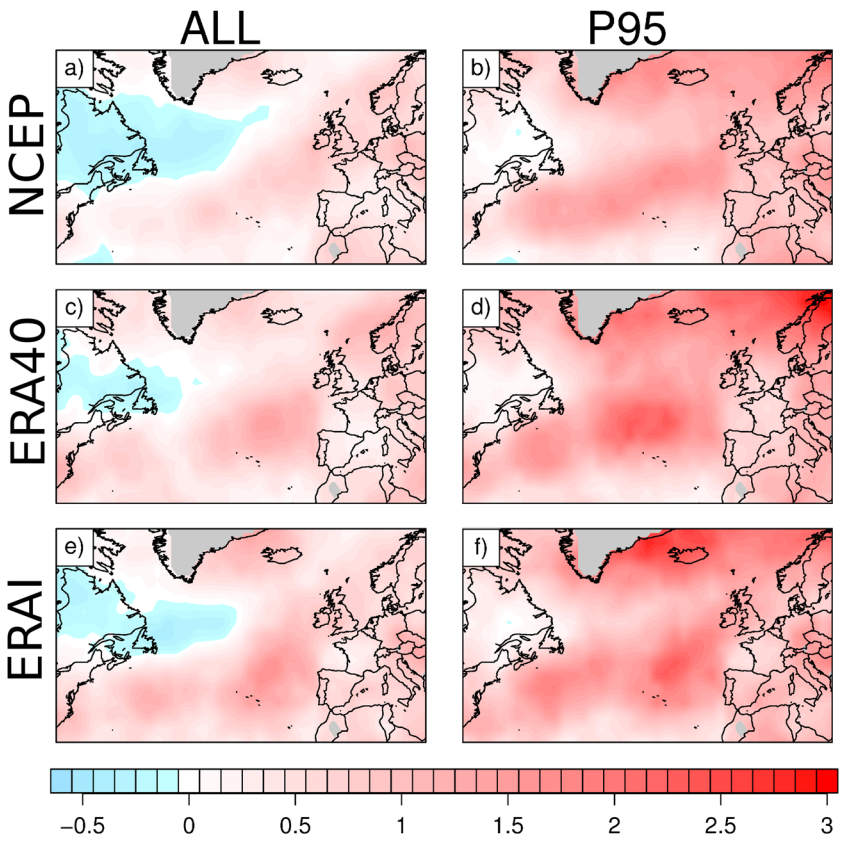

Figure 3. (a) Estimated dispersion statistic (Ψ) for NCEP for the winter cyclone transits (December–February) for all cyclones and the period 1948–2012. (b) Same as Figure 3a but for cyclones with minimum core pressure exceeding the 95th percentile. (c) Same as Figure 3a but for ERA-40 for the period 1958–2002. (d) Same as Figure 3c but for cyclones with minimum core pressure exceeding the 95th percentile. (e) Same as Figure 3a but for ERAI for the period 1979–2011. (f) Same as Figure 3e but for cyclones with minimum core pressure exceeding the 95th percentile. ERA40 and ERAI data were spectrally degraded to T62 to enable direct comparison. Values in areas with orography above 1500 m are suppressed. Blue values correspond to an underdispersive process ($\Psi < 0$; regular), white values to a random process ($\Psi = 0$), and red values to an overdispersive process ($\Psi > 0$; clustering).

large, cyclones may be included that do not have an immediate influence on the grid point of interest. Both examples lead to biased Ψ values. The sensitivity of Ψ as a function of radius is analyzed for the three grid points indicated in Figure 1a. Values within the range 400–1000 km are examined as they encompass the typical range of the effective radius for midlatitude cyclones, which is typically higher than 600 km over the main storm tracks but may reach up to 1000 km [*Rudeva and Gulev*, 2007]. The value 700 km was selected since this radius produced a plateau of constant values of Ψ which showed the least change at either smaller or larger radii over most of the storm track and the exit region (cf. Figure S1 in the supporting information). As an example, the corresponding area is depicted around grid point 3 in Figure 1a. In order to quantify the dependency of Ψ on cyclone intensity [*Vitolo et al.*, 2009], the 90th and 95th percentiles of MSLP values at each grid point are used as the local thresholds for cyclone core pressure for selecting the most intense cyclones. To estimate statistical significance of the results based on the 20 ECHAM5 ensemble runs, a t test is applied to the data (20 values for each grid point and each experiment, correspondent to 20 ensemble runs) to determine if the local Ψ changes are significant (5% level of significance).

3. Serial Clustering in Reanalysis Data Sets

[13] As a first step, we verify if the proposed methodology can be used to model cyclone statistics tracked with the method of *Murray and Simmonds* [1991a]. For the three selected grid points (see Figure 1a), the distribution of cyclone passages (counts) is analyzed. For grid point 3, the chosen radius and one exemplary cyclone track are depicted. By defining a cyclone passage as an event, a series of cyclone counts can be described by an inhomogeneous one-dimensional Poisson process with variable rate. The result is shown for grid point 3 and NCEP for the period December 1957 to February 1958 in Figure 1b (first row), for the whole NCEP period and for all cyclones (indicating clustering). For cyclones exceeding the 90th and 95th percentile of MSLP (Figure 1b, second and third rows), more distinct groups are identified. This general pattern is followed by the other grid points (not shown). This confirms that clustering is generally enhanced for more intense cyclones [cf. *Vitolo et al.*, 2009].

[14] The histogram in Figure 1c depicts an example of the distribution of the number of cyclones per winter (3 month period) again for NCEP and grid point 3. As a reference, the expected homogenous Poisson distribution (for the same

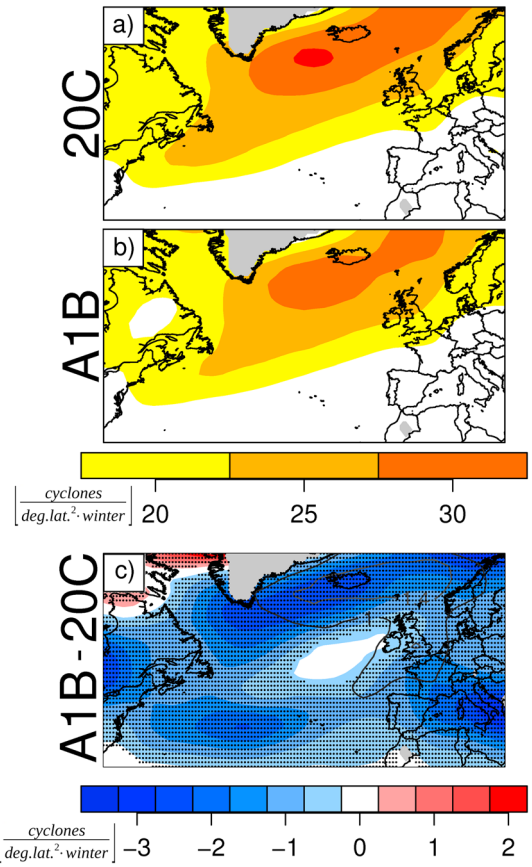

Figure 4. (a) Cyclone track density for ECHAM5 GCM ensemble average for winter season (December–February) for the period 1960–2000 (20C, 20 simulations). Values given in cyclone days per winter per (degree latitude)^2. (b) Same as Figure 4a but for the ECHAM5 GCM ensemble average for the period 2060–2100 (A1B, 20 simulations). (c) Changes in cyclone track density between Figures 4b and 4a. Blue (red) values correspond to a reduction (enhancement) of cyclone track density. Values in areas with orography above 1500 m are suppressed. Significant changes at the 5% level of significance (Student's *t* test) are areas with black stipplings. Gray isolines in Figure 4c delimit areas where spread between the GCM is large (standard deviation).

sample mean) is displayed as a curve in Figure 1c. The larger spread (variance) of the histogram compared to the Poisson distribution indicates overdispersion at grid point 3, as the variance seems to be greater than the mean of winter cyclone counts [cf. Figure 7, *Mailier et al.*, 2006], indicating that cyclones tend to occur in groups. As the chosen method seems to deliver reliable results for this grid point, it can now be applied for the whole North Atlantic area and the reanalysis data sets.

[15] First, we evaluate possible differences between the three reanalysis data sets in terms of cyclone statistics. Figure 2 shows the track density of cyclones per winter [following *Murray and Simmonds*, 1991b], which quantifies the number of cyclone tracks passing within a radius of 7.5° of a grid point within a reference period of time (here 3 months). Results of the three reanalysis data sets show similar patterns, depicting a predominance of southwest-northeast propagating cyclones over the North Atlantic storm track [e.g., *Hoskins and Valdes*, 1990]. This displays a maximum of track density to the southeast of Iceland (Figure 2a). These cyclone climatologies are similar to those produced in previous studies using this methodology [e.g., *Pinto et al.*, 2005, 2007] and other methodologies [e.g., *Hodges et al.*, 2011; *Neu et al.*, 2013]. Small differences between the data sets are likely due to the different considered time periods and also by some residual effect of resolution. Nevertheless, most of the biases related purely with resolution are avoided (cf. Figure S3 in the supporting information). The consideration of these biases is very important for the interpretation and attribution of results, as the number of cyclones is strongly dependent on spatial resolution (see section 2) and Ψ on the absolute number of counts [*Vitolo et al.*, 2009].

[16] Figure 3 shows that reanalyses produce similar Ψ values for all three data sets. For all cyclones (Figure 3, left row), regions with underdispersion ($\Psi < 0$, in blue) predominate at the entrance of the North Atlantic storm track (grid point 1 in Figure 1a), where a strong and semipermanent upper air jet stream is typically found during winter. The presence of the polar jet and thus of baroclinic instability ensures the necessary preconditioning for cyclone development over this area [e.g., *Hoskins and Valdes*, 1990; *Pinto et al.*, 2009; *Dacre and Gray*, 2009, 2013]. Therefore, the passage of cyclones over this area is recurrent (regular process). Overdispersion ($\Psi > 0$, in red) dominates for the exit region and both flanks of the storm track (grid point 3 in Figure 1a; Figures 3a, 3c, and 3e), indicating clustering. Between these areas, Ψ values are near to zero (grid point 2 in Figure 1a), which indicates serial randomness of cyclones occurrences. Also of interest is the relative minimum of clustering over France and the western Mediterranean, which may be attributed to the recurrent cyclogenesis over the western Mediterranean during wintertime [cf. *Trigo et al.*, 1999]. The present results based on three reanalysis data sets provide evidence that the pattern of clustering is a robust feature, confirming the general assessment by *Mailier et al.* [2006] based on dispersion statistics of monthly cyclone counts for NCEP.

[17] For extreme cyclones, the (red) areas displaying serial clustering are strongly enlarged, and dispersion statistics values are enhanced for the whole area, covering now most of the eastern North Atlantic and Europe (Figures 3b, 3d, and 3f). The maxima of serial clustering are located between Greenland and Iceland and from the south of Newfoundland toward western Europe. This result extends the assessment by *Vitolo et al.* [2009] that serial clustering increases for intense cyclones, as it shows that this is the case not only near and over western Europe but actually over the whole study area. However, care must be taken when interpreting the Ψ values south of 40°N, as the statistics are calculated on a small number of events (Figure 2), and thus, they are less reliable [cf. also *Mailier*, 2007]. The general pattern of dispersion statistics for NCEP, ERA-40, and ERAI are similar except in minor details that are explained by the different time periods considered for the three data sets. The results become even more coherent if Ψ values are depicted for the common time frame (1979–2002, cf. Figure S2 in the supporting information). Conversely, results are more diverse if dispersion statistic is computed based on cyclone tracks computed with the original resolution of ERA-40 and ERAI (Figure S3 in the supporting information).

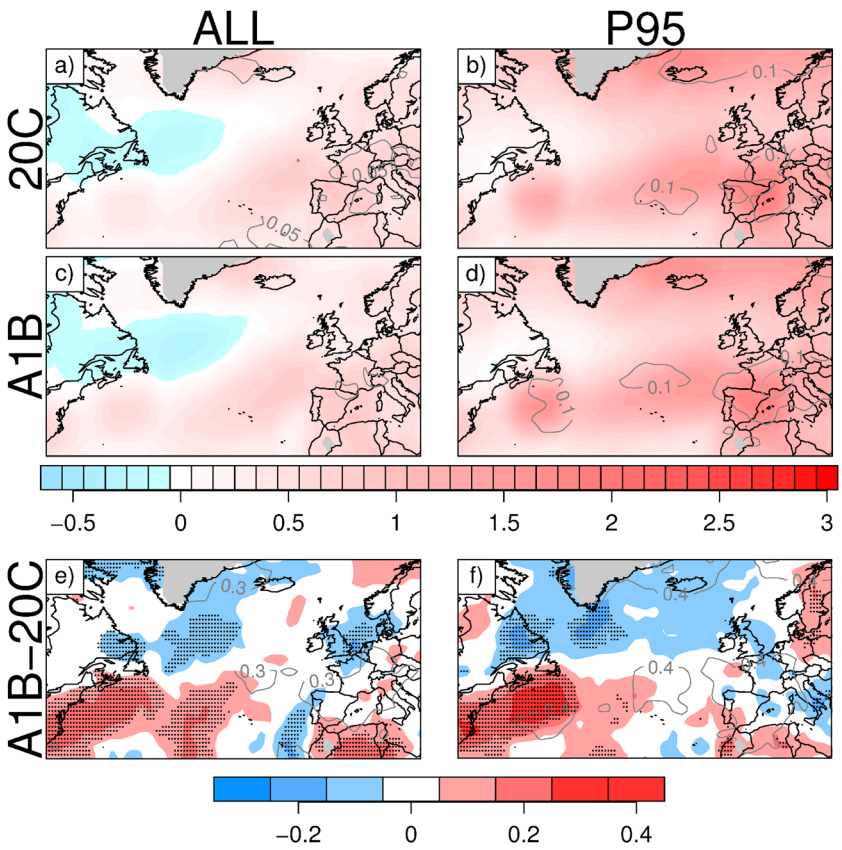

Figure 5. (a) Estimated dispersion statistic (Ψ) of winter cyclone transits (December–February) for ECHAM5 GCM ensemble average for the period 1960–2000 (20C, 20 simulations). (b) Same as Figure 5a but for cyclones with minimum core pressure exceeding the 95th percentile. (c) Same as Figure 5a but for the ECHAM5 GCM ensemble average for the period 2060–2100 (A1B, 20 simulations). (d) Same as Figure 5c but for cyclones with minimum core pressure exceeding the 95th percentile. Blue values correspond to an underdispersive process ($\Psi < 0$; regular), white values to a random process ($\Psi = 0$), and red values to an overdispersive process ($\Psi > 0$; clustering). (e) Changes in Ψ between Figures 5c and 5a. Colored areas indicate decreases (blue) or increases (red) of Ψ, statistically significant changes at the 5% level of significance (Student's *t* test) are marked with black dots. Gray isolines delimit areas where the spread between the GCM ensemble runs is high. (f) Same as Figure 5e but changes between Figures 5d and 5b.

[18] To summarize, the cyclogenetic regions at the entrance and the core area of the North Atlantic storm track are characterized by a recurrent occurrence of events (regular process). The exit area and the flanks of the North Atlantic storm track are marked by clustering of events. Here the steering through the North Atlantic Oscillation and secondary cyclogenesis play an important role. As these results are consistent with those of *Mailier et al*. [2006] and *Vitolo et al*. [2009], which used a different counting approach and a different tracking methodology [*Hodges*, 1995], we conclude that the identified pattern of clustering is a robust feature and that our methodology is suitable for evaluating serial clustering of cyclones over the North Atlantic and Europe.

4. Serial Clustering in GCM Data Sets

[19] In this section, we analyze (a) the extent to which clustering of extratropical cyclones is represented in GCMs and (b) if clustering is affected by increasing greenhouse gas concentrations. A large ensemble of ECHAM5 simulations is investigated to allow an evaluation of uncertainties and to sample decadal variability.

[20] First, the cyclone tracking results for recent (20C) and future (A1B) climate conditions are assessed (Figure 4). Cyclone track density for 20C has a similar shape and orientation to the reanalysis data sets (Figure 2), except for a zonal bias leading to an increased number of cyclones over the British Isles and nearby areas [see also *Pinto et al.*, 2007; *Zappa et al*., 2013b]. This zonal bias is associated with the deficiencies in the representation of blocking [e.g., *Sillmann and Croci-Maspoli*, 2009; *Anstey et al*., 2013]. For future climate conditions, the shape remains similar, but the total numbers are reduced (Figure 4b). This can be easily identified in Figure 4c which shows the differences between future (Figure 4b) and recent climate conditions (Figure 4a). In fact, the number of cyclones is reduced over most of the study area, primarily over the storm track area, south of Newfoundland and over the Mediterranean. However, numbers hardly change in the region to the west of and over the British Isles. This pattern of change is in agreement with previous studies [e.g., *Pinto et al*., 2007; *Ulbrich et al*., 2009; *Zappa et al*., 2013b].

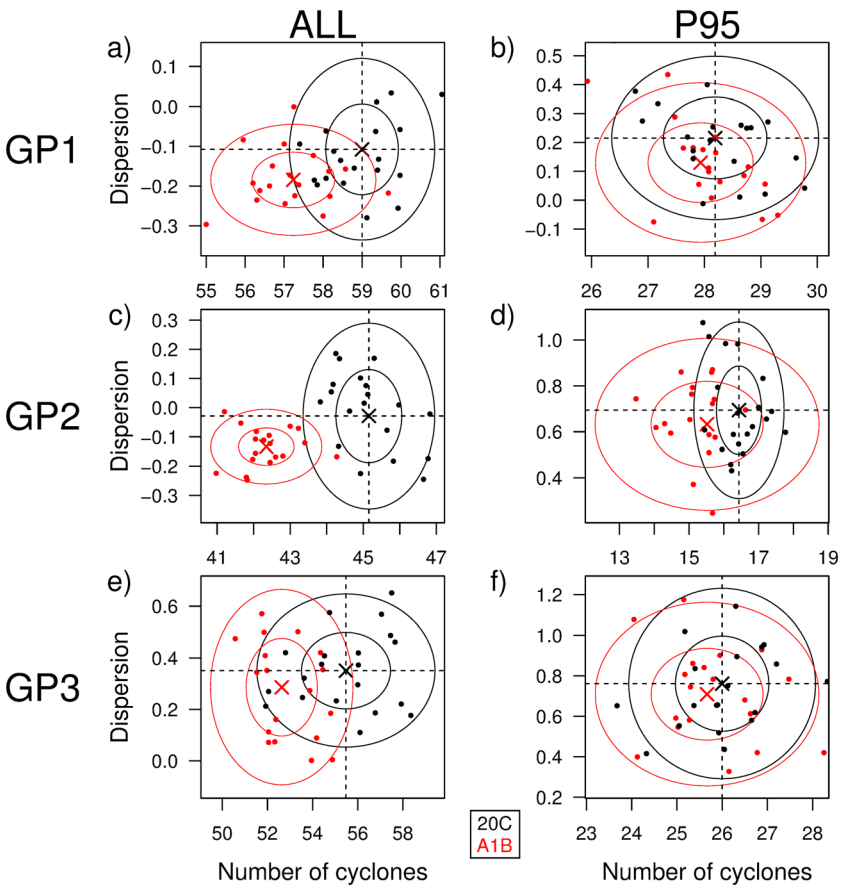

Figure 6. Scatterplots for the dispersion against the number of cyclones per winter. Black dots indicate single runs (ensemble members) for present climate conditions (1960–2000). Red dots represent single runs for future climate conditions (2060–2100). The inner circles for each color illustrate the standard deviation; the outer circle illustrates the doubled standard deviation with respect to the correspondent mean. (a) Grid point 1 (52.5°N, 55°W) regarding all cyclones. (b) Same as Figure 6a but with minimum core pressure exceeding the 95th percentile. (c) Same as Figure 6a but for grid point 2 (55°N, 30°W). (d) Same as Figure 6d but for grid point 2. (e) Same as Figure 6a but for grid point 3 (55°N, 5°W). (f) Same as Figure 6b but for grid point 3.

Considering the uncertainty of the pattern in Figure 4c, quantified as the standard deviation between the 20 patterns for A1B minus 20C (one value per ensemble run), it is largest for the northern flank of the storm track and downstream over western Europe (cf. gray line in Figure 4c). On the other hand, the identified changes at lower latitudes are more consistent between the runs.

[21] As ECHAM5 is able to largely reproduce the cyclone climatology as identified in reanalysis data, clustering is now quantified. First, the ensemble mean of the dispersion statistic for the recent climate (20C; Figure 5a) is found to reproduce the general patterns of the reanalysis data (Figure 3): serial regularity is identified at the entrance and core area of the main storm track and serial clustering in the downstream region and flanks of the storm track. Furthermore, the Ψ values for 20C clearly show an increase of serial clustering for stronger cyclones for almost all of the study area (Figure 5b). Nevertheless, biases compared to Figure 3 are clear: the areas of enhanced clustering on both flanks of the storm track have a more zonal orientation and extend too far east, particularly over western Europe. This leads to an unrealistic local maximum near the Spanish/French Mediterranean coastal areas. These biases are qualitatively similar to those identified by *Kvamsto et al.* [2008] for the ARPEGE model under recent climate conditions and may be attributed to the more zonal orientation of the polar jet in GCMs [e.g., *Pinto et al.*, 2007; *Delcambre et al.*, 2013a; *Zappa et al.*, 2013a] related to the biases in blocking [e.g., *Anstey et al.*, 2013].

[22] For future climate conditions, the general pattern of dispersion statistic does not change considerably (Figures 5c and 5d). Regularity generally increases poleward of 50°N (blue areas in Figure 5e) with significant reductions identified over the entrance region of the storm track, south of Greenland and over British Isles (Figure 5e, black stipplings indicate significant changes at the 5% level of significance). These changes may be attributed to an intensification and downstream extension of the eddy-driven jet under future climate conditions [e.g., *Pinto et al.*, 2007; *Woollings et al.*, 2012; *Delcambre et al.*, 2013b], enabling a more regular occurrence of cyclones over this area. The jet changes are associated with a northeastward shift of the blocking pattern under future climate conditions [*Sillmann and Croci-Maspoli*, 2009].

[23] A significant increase in clustering can be found south of 50°N (especially south of Newfoundland, cf. red areas

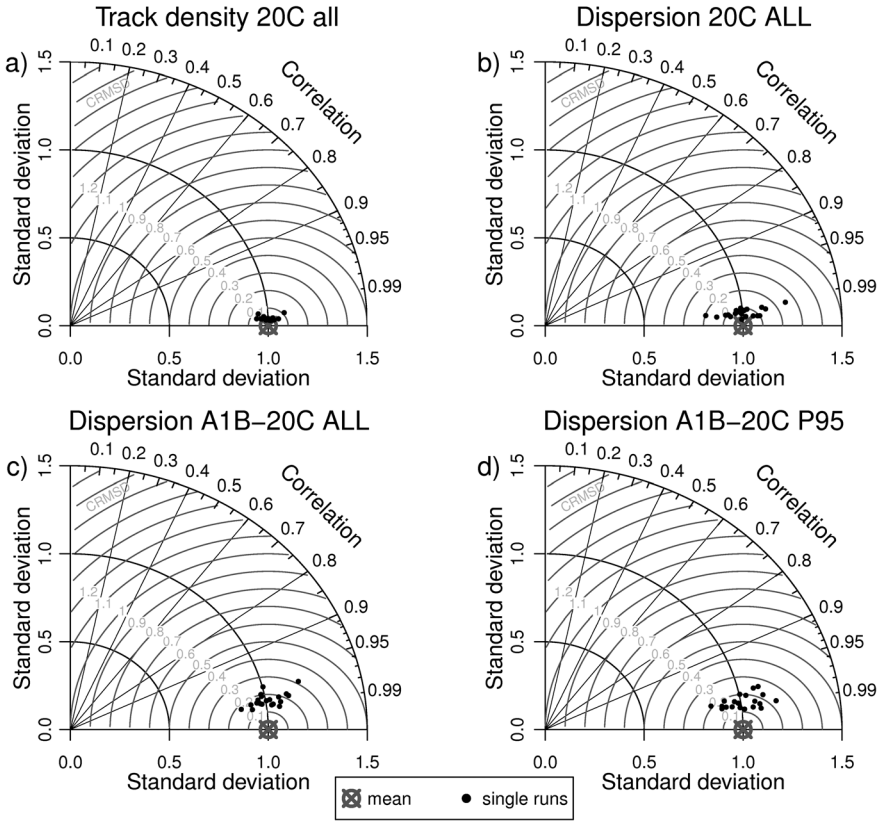

Figure 7. Taylor diagrams indicating the standard deviation, the correlation coefficient, and the centered root mean square for single runs. Black dots imply single runs; the gray cross represents the mean of all runs. (a) Track density for present climate conditions (1960–2000) taking account of all cyclones within the winter period. (b) Same as Figure 7a but for the dispersion statistic (Ψ) (c) Difference of the dispersion statistic between the future climate conditions (2060–2100) and present climate conditions (1960–2000) considering all cyclones. (d) Same as Figure 7c but including only cyclones with minimum core pressure exceeding the 95th percentile.

with black stipplings in Figure 5e). Regarding intense cyclones, Ψ values decrease particularly over the entrance region of the storm track and south of Greenland (Figure 5f). However, the decrease of Ψ values further downstream and over western Europe is not statistically significant. On the other hand, Ψ values increase for extreme cyclones south of Newfoundland, which could be related with changes in cyclogenesis over this region (not shown). Cyclones over this area are more sensitive to the local baroclinicity than cyclones in the downstream region of the North Atlantic storm track [e.g., *Dacre and Gray*, 2013], which may explain the different behavior in terms of the changes in dispersion statistics. This difference may also be associated with the pronounced minimum in surface warming in the North Atlantic (cf. *Woollings et al*., 2012, their Figure 3a), which leads to enhanced (reduced) temperature gradients south (north) of the main storm track axis [cf. also *Harvey et al*., 2013]. The physical factors contributing to this behavior should be analyzed in detail in future studies. As mentioned above, the dispersion statistic estimates south of 40°N and thus their changes may be regarded as more uncertain.

[24] In order to estimate the statistical uncertainty of the results, we analyze first the spread between the single runs for the three representative grid points (cf. Figure 1a). Results for all grid points show a similar pattern (Figure 6) and confirm the general tendencies observed in Figure 5. Considering all cyclones, the ensemble mean for 2060–2100 has both fewer cyclones and lower dispersion than 20C, leading to a shift of the distributions to the lower left corner (Figures 6a, 6c, and 6e, bold red and black dots). This indicates both less cyclones and reduced clustering under future climate conditions. For the A1B scenario period, the spread between the 20 individual runs (indicated as single red dots) is smaller than for 20C (black dots). Considering only extreme cyclones (Figures 6b, 6d, and 6f), the tendencies are similar. However, the spread (depicted as circles of 1 and 2 standard deviations) between the single runs for A1B is similar to 20C (unlike for all cyclones).

[25] To evaluate the consistency of the results over the whole study area, the Taylor diagrams in Figure 7 show the spread between the 20 individual runs compared to the ensemble mean. Considering the cyclone track density, results show an excellent agreement between the patterns, with a standard deviation for the single runs between 0.9 and 1.1 (Figure 7a). The correlation between the single runs and the mean is higher than 0.99, which means that the track density has little spread between the runs. For dispersion statistics (Figure 7b), the results are similar, but the standard deviation is slightly higher (0.8–1.25). In spatial terms, the main differences between the runs are identified between Iceland and Norway, over western Europe and west of Iberia for extreme

cyclones (see lines in Figure 5b). Regional differences for all cyclones have a comparable pattern but are weaker (Figure 5a).

[26] The standard deviation of the climate change signal of all cyclones (Figure 7c) is about 0.8–1.35, and the correlation is between 0.95 and 0.99. The results for extreme cyclones are similar (Figure 7d), demonstrating the general consistency of the outcome. All single runs show basically the same spatial pattern, but small differences in terms of the magnitude are found. In regional terms, the largest spread between the runs are identified for western and southwestern Europe (Figure 5f), with larger changes for extreme cyclones. This may be associated with the uncertainty of dispersion statistics for the A1B scenario period over this area for extreme cyclones (Figure 5d). In summary, the GCM ensemble provides a consistent and robust pattern of change, which indicates that clustering may change over North Atlantic and Europe under future climate conditions. Yet the tendencies are often not statistically significant.

5. Conclusions

[27] We have adapted a method to quantify serial clustering of windstorms and analyzed its dependency on cyclone intensity for the North Atlantic/western Europe. Results show that serial clustering is found primarily on the flanks and downstream regions of the dominant North Atlantic storm track and that this pattern is a robust feature in the reanalysis data sets. Extreme cyclones show a higher magnitude of serial clustering. This is true not only for western Europe but also for the North Atlantic area. These results confirm and extend those presented in previous studies using a different methodology [*Mailier et al*., 2006; *Vitolo et al*., 2009]. The present results provide further evidence of the adequacy of the methodology to model cyclone clustering from cyclone track data. Nevertheless, the sensitivity to the choice of the tracking method should be further considered, e.g., within the scope of the Intercomparison of Midlatitude Storm diagnostics initiative [cf. *Neu et al*., 2013].

[28] The analysis of a large coupled GCM ensemble for current climate conditions shows that the GCM is generally able to reproduce the spatial patterns of serial characteristics of cyclone events, but some biases occur. For example, the areas of serial clustering display higher zonality than in the reanalyses, and dispersion statistics values are positively biased over Iberia, France, and the western Mediterranean. Comparable biases have been identified in the previous studies focusing on GCM data for recent climate conditions [*Mailier*, 2007; *Kvamsto et al*., 2008]. Under future climate conditions, the GCM ensemble indicates that serial clustering generally decreases over the North Atlantic storm track area and over parts of western Europe, also for extreme cyclones. On the other hand, an increase of clustering south of Newfoundland is identified. In both cases, these tendencies are often not statistically significant. Nevertheless, the coherence of results between the 20 ensemble runs is high, demonstrating the robustness of the results. The largest spread between ensemble members, in terms of the climate signal, is found for southwestern Europe, an area of great relevance for the potential societal impacts (e.g., the insurance losses caused by wind damage to property). Insured losses associated with windstorms have been explicitly estimated using wind speed or wind speed gusts [e.g., *Klawa and Ulbrich*, 2003]. Using this approach, potential losses for western Europe have been projected to increase under future climate conditions, with significantly shorter return periods for individual countries like France and Germany [cf. *Donat et al*., 2011; *Pinto et al*., 2012]. Current generation windstorm loss models [cf. *Haylock*, 2011] consider serial clustering based on observed values of dispersion statistic presented here. These models should be run with projected increases in windstorm intensity together with the decreases in clustering given by this study to quantify the effects of both on the risk of loss.

[29] The uncertainty of the impact of climate change on serial clustering of extratropical cyclones may be underestimated, as the present study considered only a single GCM, though with a large 20-member ensemble. Therefore, it will be important to analyze possible changes in clustering based on the multimodel CMIP5 ensemble to estimate the uncertainties related with the model architecture and complexity and also to take newer forcing scenarios into account.

[30] **Acknowledgments.** We thank the European Centre for Medium-Range Weather Forecasts and the National Centers for Environmental Prediction/National Center for Atmospheric Research for the various reanalysis data sets. We thank the MPI (Hamburg, Germany) for the MPI-ECHAM5 data, Andreas Sterl from KNMI (De Bilt, Netherlands) for the ESSENCE data, and the DKRZ/WDCC and ZAIK/RRZK for computer and storage capacity. J. G. Pinto was supported by the German Federal Ministry of Education and Research (BMBF) under the project "Probabilistic Decadal Forecast for Central and western Europe" (MIKLIP-PRODEF, contract 01LP1120A). We thank Helen F. Dacre (University of Reading) and Sven Ulbrich (University of Cologne) for discussions. We also thank three anonymous reviewers for their helpful and constructive comments.

References

Anstey, J. A., P. Davini, L. J. Gray, T. J. Woollings, N. Butchart, C. Cagnazzo, B. Christiansen, S. C. Hardiman, S. M. Osprey, and S. Yang (2013), Multi-model analysis of Northern Hemisphere winter blocking: Model biases and the role of resolution, *J. Geophys. Res. Atmos.*, *118*, 3956–3971, doi:10.1002/jgrd.50231.

Bader, J., M. D. S. Mesquita, K. I. Hodges, N. Keenlyside, S. Østerhus, and M. Miles (2011), A review on Northern Hemisphere sea ice, storminess and the North Atlantic Oscillation: Observations and projected changes, *Atmos. Res.*, *101*, 809–834.

Bengtsson, L., K. I. Hodges, and E. Roeckner (2006), Storm tracks and climate change, *J. Clim.*, *19*, 3518–3543.

Bjerknes, J., and H. Solberg (1922), Life cycle of cyclones and the polar front theory of atmospheric circulation, *Geofys. Publ.*, *3*, 3–18.

Cox, D. R., and V. Isham (1980), *Point Processes*, pp. 188, Chapman and Hall/CRC, London.

Dacre, H. F., and S. L. Gray (2009), The spatial distribution and evolution characteristics of North Atlantic cyclones, *Mon. Weather Rev.*, *137*, 99–115.

Dacre, H. F., and S. L. Gray (2013), Quantifying the climatological relationship between extratropical cyclone intensityand atmospheric precursors, *Geophys. Res. Lett.*, *40*, 2322–2327, doi:10.1002/grl.50105.

Dee, D., et al. (2011), The ERA-Interim reanalysis: Configuration and performance of the data assimilation system, *Q. J. R. Meteorol. Soc.*, *137*, 553–597.

Delcambre, S. C., D. J. Lorenz, D. J. Vimont, and J. E. Martin (2013a), Diagnosing Northern Hemisphere jet portrayal in 17 CMIP3 global climate models: Twentieth-century intermodel variability, *J. Clim.*, *26*, 4910–4929.

Delcambre, S. C., D. J. Lorenz, D. J. Vimont, and J. E. Martin (2013b), Diagnosing Northern Hemisphere jet portrayal in 17 CMIP3 global climate models: Twenty-first-century projections, *J. Clim.*, *26*, 4930–4946.

Della-Marta, P. M., and J. G. Pinto (2009), Statistical uncertainty of changes in winter storms over the North Atlantic and Europe in an ensemble of transient climate simulations, *Geophys. Res. Lett.*, *36*, L14703, doi:10.1029/2009GL038557.

Della-Marta, P. M., H. Mathis, C. Frei, M. A. Liniger, J. Kleinn, and C. Appenzeller (2009), The return period of wind storms over Europe, *Int. J. Climatol.*, *29*, 437–437, doi:10.1002/joc.1794.

Della-Marta, P. M., M. A. Liniger, C. Appenzeller, D. N. Bresch, P. Köllner-Heck, and V. Muccione (2010), Improved estimates of the European winter windstorm climate and the risk of reinsurance loss using climate model data, *J. Appl. Meteorol. Climatol.*, *49*, 2092–2120.

Donat, M. G., G. C. Leckebusch, S. Wild, and U. Ulbrich (2011), Future changes of European winter storm losses and extreme wind speeds in multi-model GCM and RCM simulations, *Nat. Hazards Earth Syst. Sci.*, *11*, 1351–1370.

Fink, A. H., T. Brücher, E. Ermert, A. Krüger, and J. G. Pinto (2009), The European storm Kyrill in January 2007: Synoptic evolution, meteorological impacts and some considerations with respect to climate change, *Nat. Hazards Earth Syst. Sci.*, *9*, 405–423.

Franzke, C. L. E. (2013), Persistent regimes and extreme events of the North Atlantic atmospheric circulation, *Phil. Trans. R. Soc. A*, *371*, 20110471, doi:10.1098/rsta.2011.0471.

Harvey, B. J., L. C. Shaffrey, T. J. Woollings, G. Zappa, and K. I. Hodges (2012), How large are projected 21st century storm track changes?, *Geophys. Res. Lett.*, *39*, L18707, doi:10.1029/2012GL052873.

Harvey, B. J., L. C. Shaffrey, and T. J. Woollings (2013), Equator-to-pole temperature differences and the extra-tropical storm track responses of the CMIP5 climate models, *Clim. Dyn.*, doi:10.1007/s00382-013-1883-9, in press.

Haylock, M. R. (2011), European extra-tropical storm damage risk from a multimodel ensemble of dynamically-downscaled global climate models, *Nat. Hazards Earth Syst. Sci.*, *11*, 2847–2857.

Hodges, K. I. (1995), Feature tracking on the unit sphere, *Mon. Weather Rev.*, *123*, 3458–3465.

Hodges, K. I., R. W. Lee, and L. Bengtsson (2011), A comparison of extratropical cyclones in recent reanalyses ERA-interim, NASA MERRA, NCEP CFSR, and JRA-25, *J. Clim.*, *24*, 4888–4906.

Hoskins, B. J., and P. J. Valdes (1990), On the existence of storm-tracks, *J. Atmos. Sci.*, *47*, 1854–1864.

Hueging, H., K. Born, R. Haas, D. Jacob, and J. G. Pinto (2013), Regional changes in wind energy potential over Europe using regional climate model ensemble projections, *J. Appl. Meteorol. Climatol.*, *52*, 903–917.

Hurrel, J. W., Y. Kushnir, G. Ottersen, and M. Visbeck (2003), An overview of the North Atlantic Oscillation: Climatic significance and environmental impact, *Geophys. Monogr. Ser.*, vol. 134, pp. 1–35, AGU, Washington, D. C., doi:10.1029/134GM01.

Jung, T., S. K. Gulev, I. Rudeva, and V. Soloviov (2006), Sensitivity of extratropical cyclone characteristics to horizontal resolution in the ECMWF model, *Q. J. R. Meteorol. Soc.*, *132*, 1839–1857.

Jungclaus, J. H., N. Keenlyside, M. Botzet, H. Haak, J.-J. Luo, M. Latif, J. Marotzke, U. Mikolajewicz, and E. Roeckner (2006), Ocean circulation and tropical variability in the coupled model ECHAM5/MPI-OM, *J. Clim.*, *19*, 3952–3972.

Kistler, R., et al. (2001), The NCEP/NCAR 50-year reanalysis: monthly-means CDROM and documentation, *Bull. Am. Meteorol. Soc.*, *82*, 247–267.

Klawa, M., and U. Ulbrich (2003), A model for the estimation of storm losses and the identification of severe winter storms in Germany, *Nat. Hazards Earth Syst. Sci.*, *3*, 725–732.

Kvamsto, N. G., Y. Song, I. A. Seierstad, A. Sorteberg, and D. B. Stephenson (2008), Clustering of cyclones in the ARPEGE general circulation model, *Tellus Ser. A*, *60*, 547–556.

Mailier, P. J. (2007), *Serial clustering of extratropical cyclones*, PhD thesis, Univ. of Reading, United Kingdom (available at ethos.bl.uk).

Mailier, P. J., D. B. Stephenson, C. A. T. Ferro, and K. I. Hodges (2006), Serial clustering of extratropical cyclones, *Mon. Weather Rev.*, *134*, 2224–2240.

Mumby, P. J., R. Vitolo, and D. B. Stephenson (2011), Temporal clustering of tropical cyclones and its ecosystem impacts, *Proc. Natl. Acad. Sci. U. S. A.*, *108*, 17,626–17,630.

MunichRe (2010) Significant European winter storms 1980−June 2010. Overall losses. Available at www.munichre.com (in German)

Murray, R. J., and I. Simmonds (1991a), A numerical scheme for tracking cyclone centres from digital data. Part I: Development and operation of the scheme, *Aust. Meteorol. Mag.*, *39*, 155–166.

Murray, R. J., and I. Simmonds (1991b), A numerical scheme for tracking cyclone centres from digital data. Part II: Application to January and July general circulation model simulations, *Aust. Meteorol. Mag.*, *39*, 167–180.

Neu, U., et al. (2013), IMILAST – A community effort to intercompare extratropical cyclone detection and tracking algorithms, *Bull. Am. Meteorol. Soc.*, *94*, 529–547.

Parker, D. J. (1998), Secondary frontal waves in the North Atlantic region: A dynamical perspective of current ideas, *Q. J. R. Meteorol. Soc.*, *124*, 829–856.

Pinto, J. G., T. Spangehl, U. Ulbrich, and P. Speth (2005), Sensitivities of a cyclone detection and tracking algorithm: Individual tracks and climatology, *Meteorol. Z.*, *14*, 823–838.

Pinto, J. G., U. Ulbrich, G. C. Leckebusch, T. Spangehl, M. Reyers, and S. Zacharias (2007), Changes in storm track and cyclone activity in three SRES ensemble experiments with the ECHAM5/MPI-OM1 GCM, *Clim. Dyn.*, *29*, 195–210, doi:10.1007/s00382-007-0230-4.

Pinto, J. G., S. Zacharias, A. H. Fink, G. C. Leckebusch, and U. Ulbrich (2009), Factors contributing to the development of extreme North Atlantic cyclones and their relationship with the NAO, *Clim. Dyn.*, *32*, 711–737.

Pinto, J. G., M. K. Karremann, K. Born, P. M. Della-Marta, and M. Klawa (2012), Loss potentials associated with European windstorms under future climate conditions, *Clim. Res.*, *54*, 1–20.

Raible, C. C. (2007), On the relation between extremes of midlatitude cyclones and the atmospheric circulation using ERA40, *Geophys. Res. Lett.*, *34*, L07703, doi:10.1029/2006GL029084.

Rind, D., J. Perlwitz, and P. Lonergan (2005), AO/NAO response to climate change: 1. Respective influences of stratospheric and tropospheric climate changes, *J. Geophys. Res.*, *110*, D12107, doi:10.1029/2004JD005103.

Rivals, H., J.-P. Cammas, and I. A. Renfrew (1998), Secondary cyclogenesis: The initiation phase of a frontal wave observed over the eastern Atlantic, *Q. J. R. Meteorol. Soc.*, *124*, 243–267.

Rudeva, I., and S. K. Gulev (2007), Climatology of cyclone size characteristics and their changes during the cyclone life cycle, *Mon. Weather Rev.*, *135*, 2568–2587.

Schwierz, C., E. Zenklusen Mutter, P.-L. Vidale, M. Wild, C. Schär, P. Köllner-Heck, and D. N. Bresch (2010), Modelling European winter wind storm losses in current and future climate, *Clim. Change*, *101*, 485–514.

Seierstad, I. A., D. B. Stephenson, and N. G. Kvamsto (2007), How useful are teleconnection patterns for explaining variability in extratropical storminess?, *Tellus Series A*, *59*, 170–181.

Sillmann, J., and M. Croci-Maspoli (2009), Present and future atmospheric blocking and its impact on European mean and extreme climate, *Geophys. Res. Lett.*, *36*, L10702, doi:10.1029/2009GL038259.

Stephenson, D. B., V. Pavan, M. Collins, M. M. Junge, and R. Quadrelli (2006), North Atlantic Oscillation response to transient greenhouse gas forcing and the impact on European winter climate: A CMIP2 multi-model assessment, *Clim. Dyn.*, *27*, 401–420, doi:10.1007/s00382-006-0140-x.

Sterl, A., C. Severijns, H. Dijkstra, W. Hazeleger, G. Jan van Oldenborgh, M. van den Broeke, G. Burgers, B. van den Hurk, P. Jan van Leeuwen, and P. van Velthoven (2008), When can we expect extremely high surface temperatures?, *Geophys. Res. Lett.*, *35*, L14703, doi:10.1029/2008GL034071.

Taylor, K. E., R. J. Stouffer, and G. A. Meehl (2012), An overview of CMIP5 and the experiment design, *Bull. Am. Meteorol. Soc.*, *93*, 485–498.

Trigo, I. F., T. D. Davies, and G. R. Bigg (1999), Objective climatology of cyclones in the Mediterranean region, *J. Clim.*, *12*, 1685–1696.

Ulbrich, U., J. G. Pinto, H. Kupfer, G. C. Leckebusch, T. Spangehl, and M. Reyers (2008), Changing Northern Hemisphere storm tracks in an ensemble of IPCC climate change simulations, *J. Clim.*, *21*, 1669–1679.

Ulbrich, U., G. C. Leckebusch, and J. G. Pinto (2009), Cyclones in the present and future climate: A review, *Theor. Appl. Climatol.*, *96*, 117–131.

Uppala, S. M., et al. (2005), The ERA40 re-analysis, *Q. J. R. Meteorol. Soc.*, *131*, 2961–3012.

Vitolo, R., D. B. Stephenson, I. M. Cook, and K. Mitchell-Wallace (2009), Serial clustering of intense European storms, *Meteorol. Z.*, *18*, 411–424.

Woollings, T., J. M. Gregory, J. G. Pinto, M. Reyers, and D. J. Brayshaw (2012), Response of the North Atlantic storm track to climate change shaped by ocean–atmosphere coupling, *Nat. Geosci.*, *5*, 313–317.

Zappa, G., L. C. Shaffrey, and K. I. Hodges (2013a), The ability of CMIP5 models to simulate North Atlantic extratropical cyclones, *J. Clim.*, *26*, 5379–5396.

Zappa, G., L. C. Shaffrey, K. I. Hodges, P. G. Sansom, and D. B. Stephenson (2013b), A multi-model assessment of future projections of North Atlantic and European extratropical cyclones in the CMIP5 climate models, *J. Clim.*, *26*, 5846–5862.